International Immunopharmacology 74 (2019) 105685

Contents lists available at ScienceDirect

International Immunopharmacology

journal homepage: www.elsevier.com/locate/intimp

BMP9 inhibits the proliferation and migration of fibroblast-like synoviocytes in rheumatoid arthritis via the PI3K/AKT signaling pathway

Biao Song[a,b], Xiao-Feng Li[a,b], Yao Yao[a,b], Qing-Qing Xu[a,b], Xiao-Ming Meng[a,b], Cheng Huang[a,b], Jun Li[a,b,*]

[a] Anhui Province Key Laboratory of Major Autoimmune Diseases, Anhui Institute of Innovative Drugs, School of Pharmacy, Anhui Medical University, Hefei 230032, China
[b] The Key Laboratory of Anti-inflammatory and Immune medicines, Ministry of Education, Hefei 230032, China

ARTICLE INFO

Keywords:
Adjuvant-induced arthritis
BMP9
Proliferation
Migration

ABSTRACT

Rheumatoid arthritis (RA) is a chronic autoimmune inflammatory disease; its pathogenesis remains unclear. Fibroblast-like synoviocytes (FLSs) play a vital role in the pathogenesis of RA. BMP9, a member of the bone morphogenetic protein (BMP) family, has been reported to play a critical role in both normal physiological processes and the pathology of various diseases. In this study, we explored the function and underlying mechanisms of BMP9 in the proliferation and migration of RA FLSs. We found that BMP9 expression was significantly downregulated in the synovial tissues of RA patients, compared with those of OA patients; BMP9 expression was also low in adjuvant-induced arthritis (AA) samples. Additionally, inhibition of BMP9 expression by BMP9 siRNA increased the proliferation of AA FLSs, and the expression of c-Myc, Cyclin D1, MMP-2, and MMP-9, but not TIMP-1, in AA FLSs. However, AA FLSs transfected with the overexpression vector PEX-3-BMP9 showed reduced proliferation and expression of c-Myc, Cyclin D1, MMP-2, and MMP-9, but not TIMP-1. Further studies indicate that BMP9 may induce the activation of the PI3K/AKT signaling pathway. Thus, these data indicate that BMP9 may play a critical role in the proliferation and migration of FLSs through the activation of the AKT signaling pathway.

1. Introduction

Rheumatoid arthritis (RA) is a chronic inflammatory immune-mediated disorder; synovial hyperplasia, pannus formation, and the subsequent erosion of adjacent articular cartilage and bone are the histological features of RA [1,2]. The pathogenesis of RA involves a variety of RA-related inflammatory cells, such as T lymphocytes, B lymphocytes, fibroblast-like synoviocytes (FLSs), and macrophages [3]. Interestingly, FLSs are located at the junction of the knee joint, and play an important role in the pathogenesis of RA [4,5]. In the RA synovium, activated FLSs actively participate in the inflammatory processes of RA by producing the pro-inflammatory cytokines TNF-α and IL-6 [1,6], angiogenic factors, and matrix metalloproteinases (MMPs) [7]. The sustained stimulation of synovial cells, resulting in the continuous activation of intracellular protein kinases, finally leading to abnormal signal transduction and the proliferation of synoviocytes [8]. Thus, the inhibition of FLS proliferation is an ideal target for the treatment of RA.

Bone morphogenetic proteins (BMPs), which were originally introduced by Urist, can induce the ectopic formation of bone marrow cartilage and bone tissue [9,10]. BMPs are members of the transforming growth factors β (TGF-β) superfamily [11]. An increasing number of studies believe that BMPs not only play a pivotal role in bone development and repair regeneration, but also participate in regulating embryonic development and organogenesis, and regulating the growth, development, apoptosis, migration, and invasion of various tissue cells [12–14]. In recent years, evidence has suggested that BMP signaling pathways are activated in the synovial membranes of RA patients and collagen-induced rheumatoid arthritis (CIA) models [15,16]. Furthermore, BMP2 and TGF-β1 inhibit the expression of the pro-inflammatory cytokine IL-34 in RA synovial fibroblasts [17]. These findings indicate that BMPs result in the development of RA.

BMP9, also known as growth differentiation factor 2, has the strongest osteogenic effect of all BMPs [18]. More recently, BMP9 has been demonstrated to play different roles in different tumors. BMP9 has also been shown to inhibit the proliferation, migration, and invasiveness of osteosarcoma [19] and breast cancer cells [20], but promote the proliferation and migration of liver and bladder cancer cells [21,22]. In addition, the anti-inflammatory effect of BMP9 has been confirmed in

* Corresponding author at: Anhui Province Key Laboratory of Major Autoimmune Diseases, Anhui Institute of Innovative Drugs, School of Pharmacy, Anhui Medical University, Hefei 230032, China.
E-mail address: lj@ahmu.edu.cn (J. Li).

https://doi.org/10.1016/j.intimp.2019.105685
Received 19 April 2019; Received in revised form 17 May 2019; Accepted 5 June 2019
Available online 13 June 2019

vitro [23]. Nevertheless, the role of BMP9 in RA has not yet been reported. Therefore, it is of great significance to explore whether BMP9 is related to RA.

We first performed vital experiments and surprisingly found that the expression of BMP9 was aberrantly downregulated in the FLSs from rats with adjuvant-induced arthritis (AA), compared to that of the rats from the normal group. Silencing BMP9 promoted the proliferation and migration of FLSs. Similarly, the overexpression of BMP9 was negatively correlated with the proliferation and migration response of FLSs. In addition, we found that the AKT pathway is associated with the expression of BMP9 in AA FLSs. Collectively, these results indicate that BMP9 inhibits the proliferation and migration of FLSs in AA, which may be closely related to the AKT signaling pathway.

2. Materials and methods

2.1. Materials and reagents

Complete Freund's Adjuvant (CFA) was purchased from Sigma-Aldrich (St. Louis, MO, USA). Fetal bovine serum (FBS) was obtained from Gibco (USA). High-glucose Dulbecco's modified Eagle's medium (DMEM) was acquired from Hyclone (Logan, UT, USA). Rabbit anti-BMP9 and anti-TIMP metallopeptidase inhibitor 1 (TIMP-1) antibodies were purchased from Abcam (Cambridge, UK). Rabbit anti-c-Myc and anti-CyclinD1 antibodies were purchased from Cell Signaling (Danvers, MA, USA). Rabbit anti-MMP9 and anti-MMP2 antibodies were purchased from Merck Millipore (Billerica, MA). Rat anti-β-actin antibodies were purchased from Bioworld (Shanghai, China). Secondary antibodies for goat anti-rabbit and goat anti-mouse immunoglobulin (IgG)-horse radish peroxidase (HRP) were procured from Zhong-shan (Beijing, China). BMP9, MMP2, MMP9, TIMP-1, c-Myc, cyclinD1, and β-actin primers were synthesized by the Shanghai Sangon Biological and Technological Company (Shanghai, China).

2.2. Human synovial tissue collection

The synovial tissue was obtained from patients with RA ($n = 5$) according to the 1987 American College of Rheumatology criteria (revised) during joint synovectomies; patients with osteoarthritis (OA, n = 5) served as the controls. All patients signed the informed consent forms to participate in the study. The study protocol was approved by the ethics board of the Anhui Medical University, and tissue specimen acquisition was performed in accordance with the institutional guidelines. Written informed consent was obtained from all subjects.

2.3. AA rat models

The experimental protocols involving animals were approved by the Animal Care and Use Committee of the Anhui Medical University, China. Adult female Sprague-Dawley (SD) rats (160–200 g) were injected with 0.1 ml (5 mg/ml) of complete Freund's adjuvant (CFA) per 100 g of body weight at the left paw to induce RA. Normal rats (controls) were treated with normal saline at the same time. The animals were randomly divided into the normal group and model group ($n = 5$ per group). All animals were sacrificed at day 24 after adjuvant injection for further examination.

2.4. Histopathology

Animals were sacrificed after 24 days. Synovial tissues from patients and rats were also fixed with 4% paraformaldehyde for 24 h and then embedded in paraffin wax. Hematoxylin and eosin (H&E) staining and immunohistochemistry were performed according to standard protocols. Pathological changes were observed and photographed using the Olympus BX-51 microscope.

2.5. Cell culture

FLSs were derived from the synovial tissues of the AA model rats and control rats. The rats were killed on day 24, and the synovial tissues were promptly harvested for further experiments. Fresh synovial tissues extracted from the knee joints of the rats were minced, cultured in cell culture flasks, and maintained in high-glucose DMEM (Hyclone, USA) supplemented with 20% (*v*/v) fetal bovine serum (FBS) (Gibco, USA) and penicillin-streptomycin solution (Beyotime, China). All cell cultures were maintained at 37 °C in an atmosphere of 5% CO_2 for 7 days. After the removal of the synovial tissue blocks, the adherent cells were cultured in DMEM containing 20% FBS. The cells were trypsinized and split in a 1:2 ratio after attaining a confluence of 70–80% and cultured in DMEM containing 20% FBS. After three passages, most of the cultured synoviocytes comprised a homogeneous population of FLSs. Thus, in the following experiments, the FLSs from passage 3 were used.

2.6. Immunofluorescence staining

Cultured FLSs were plated in DMEM supplemented with 20% FBS at a density of $1–2 \times 10^5$ cells/ml. Immunofluorescence staining was performed using rabbit anti-BMP9 (Abcam, Cambridge, UK) and rabbit anti-vimentin antibodies (Cell Signaling, USA). Alexa Fluor 488-conjugated AffiniPure goat anti-rabbit IgG (H + L) (Zhongshan Biotechnology Corporation, Beijing) was used as the secondary antibody. Counterstaining of nuclei was performed with 4′,6-diamidino-2-phenylindole (DAPI; Beyotime, China). Stained FLSs were examined using an inverted fluorescence microscope (OLYMPUS IX83, Tokyo, Japan).

2.7. Small interfering RNA transfection

The cultured FLSs were transfected with 100 nM of small interfering RNAs (siRNAs) using Lipofectamine 2000 (Invitrogen, CA, USA), according to the manufacturer's instructions. The BMP9-siRNA (BMP9-RNAi) sense strand is 5′-GGAAGGAAACAUGGUCGUUTT-3′ and antisense strand is 5′-AACGACCAUGUUUCCUUCCTT-3′; the negative scrambled siRNA (NC-RNAi) sense strand is 5′-UUCUCCGAACGUGUC ACGUTT-3′ and antisense strand is 5′-ACGUGACACGUUCGGAGA ATT-3′ (GenePharma, Shanghai, China). After transfection for 6 h, we replaced the Opti-MEM with DMEM (containing 20% fetal bovine serum), and continued the cell culture for 48 h. The FLSs were then collected for the qRT-PCR, Western blot, and flow cytometry (FCM) analyses.

2.8. Plasmid construction and transfection of FLSs

Overexpression plasmid for BMP9 was generated by GenePharma Corporation (Shanghai, China). The FLSs were transfected in 6-well plates with PEX-3-BMP9 to induce the ectopic expression of BMP9, and with the empty PEX-3 vector (PEX-3) as a control. The transfection experiments were performed using LipofectamineTM 2000 (Invitrogen, USA), according to the manufacturer's instructions. After transfection at 37 °C for 6 h, Opti-MEM was replaced with DMEM containing 20% FBS, and the cells were cultured for another 48 h. The related indicators were then detected by qRT-PCR, Western blotting, and FCM analyses.

2.9. Cell cycle assay

The FLSs were seeded into 6-well plates and cultured for 48 h. Then, they were treated with BMP9-siRNA and PEX-3-BMP9 for 48 h, and fixed in 70% ethanol at 4 °C overnight. The FLSs were then centrifuged at 1000*g* for 5 min and resuspended in PBS. The cells were then stained with 0.5 ml of propidium iodine (PI) staining buffer (Beyotime, China), which contained 200 mg/ml RNase A and 50 μg/ml PI, at room temperature in the dark for 30 min. FCM was used to analyze the cell cycle.

All studies were performed in triplicate and repeated thrice.

2.10. Wound-healing assay

FLSs were seeded into 6-well plates (5.0×10^5 cells/mL/well) and cultured in DMEM containing 20% FBS for 24 h. The FLS monolayers were scratched along a straight line using a pipette tip, and the cell debris was washed thrice with PBS. Subsequently, the cells were subjected to serum deprivation and treated with BMP9-RNAi or PEX-3-BMP9 for 24 h. Then, the cells were fixed with methanol, stained with crystal violet, and observed under an Olympus BX-51 microscope.

2.11. Real-time quantitative PCR

Total RNA was extracted from the cultured FLSs (from the 3rd–5th generation) using TRIZOL reagent (Invitrogen, USA), and quantified using a Thermo Scientific NanoDrop 2000 spectrophotometer (Thermo Scientific, USA). The cDNA was then reverse transcribed using a TAKARA system (Japan). To detect the mRNA expression levels of the genes, the reaction was performed in a Pikoreal 96 real-time PCR system (Thermo Scientific, USA), according to the manufacturer's protocol using SYBR Green qPCR Master Mix (TAKARA, Japan). The primers we used are mentioned Table 1. The endogenous β-actin mRNA levels served as the internal controls, and the relative expression levels of the genes were analyzed using the $2 - \triangle\triangle Ct$ method. The first-strand cDNA was synthesized using the Prime Script RT reagent kit (Takara, JAP), according to the manufacturer's instructions. The conditions for reverse transcription conditions were as follows: 37 °C for 15 min, 85 °C for 5 s, and 37 °C for 10 min. PCR was performed using the following steps: 95 °C for 10 min, followed by 40 cycles at 95 °C for 15 s, and at 60 °C for about 1 min, using the Thermo Step One system.

2.12. Western blotting

The FLSs cultured in vitro and RA synovial tissues were lysed using the RadioImmunoprecipitation Assay (RIPA) reagent containing 1% phenylmethanesulfonyl fluoride (PMSF) (Beyotime, China). The whole-cell extracts (20 mg protein) were separated by 10%–12% sodium dodecyl sulfate-polyacrylamide gel electrophoresis (SDS-PAGE) and blotted onto PVDF membranes (Millipore, USA). After blocking with 5% milk, the membranes were incubated with the appropriate antibodies, which were diluted using an antibody dilution buffer (Beyotime, China). The primary antibodies against BMP9 (1:500), C-Myc (1:500), CyclinD1 (1:500), MMP3 (1:500), MMP9 (1:500), TIMP-1 (1:500), p-AKT (1500), and β-actin (11000) were used. After incubation with the primary antibodies, the blot was washed four times using TBS/Tween-20 and then incubated for 1 h with goat anti-mouse or rabbit horse radish peroxidase-conjugated antibodies (diluted 1:10000 using Tween-20) in TBS/Tween-20 containing 5% skim milk. After washing four times with TBS/Tween-20, the protein bands in the Western blot were detected using an ECL-chemiluminescence kit (ECL-plus, Thermo Scientific, USA).

Table 1
Primers sequences used for quantitative real-time PCR (Human).

Gene	Primer sequence
BMP9	Forward: 5′- GGAAGGAAACATGGTCGTTTAC-3′ Reverse: 5′- CATCCTGAATGTCCTGGGATAC-3′
c-Myc	Forward: 5′-TGCTCTCCGTCCTATGTTGC G-3′ Reverse: 5′-CAGTCCTGGATGATGATGTTCTTGA-3′
Cyclin D1	Forward: 5′-CAGCGGTAGGGATGAAATAGTGA-3′ Reverse: 5′-GGAATGGTTTTGGAACATGGAGA- 3′
MMP-2	Forward: 5′-AGCTGTGGACTCTAGGAGAAGGAC- 3′ Reverse: 5′-GAACACCAGAGGAAGCCGTCAC-3′
MMP-9	Forward: 5′-CACTGTAACTGGGGGCAACT-3′ Reverse: 5′-CACTTCTTGTCAGCGTCGAA-3′
TIMP-1	Forward: 5′-CATCTCTGGCC TCTGGCATC-3′ Reverse: 5′-CATAACGCTGGTATAAGGTGGTCTC-3′
β-Actin	Forward: 5′-TTCGCCATGGATGACGATATC-3′ Reverse: 5′-TAGGAGTCCTTCTGACCCATAC-3′

2.13. Statistical analysis

Data are expressed as the means ± SDs, and the results were from at least three experiments. Student-Newman-Keuls test or one-way analysis of variance (ANOVA) was used to compare the means of different values; the SPSS V17.0 software was used to evaluate the statistical significance of the differences. Differences with P values < 0.05 were considered statistically significant.

3. Results

3.1. Identification of AA models and FLSs

Morphological observation was carried out 24 days after the intradermal injection of CFA in the paws of the rats (Fig. 1A). The paw swelling scores were measured and rat arthritis scores were evaluated (Fig. 1B and C). The results showed that the secondary foot swelling in rats from the AA group was significantly higher than that in rats from the normal group. Histopathological analysis (Fig. 1D) confirmed that the AA rat model was established successfully. Moreover, we observed a remarkable increase in inflammatory cell infiltration and synovial hyperplasia in the synovial tissues from AA rats, compared to that in synovial tissues from rats in the normal group. The FLSs were identified by immunofluorescence staining assay (Fig. 1E). The FLSs showed a spindle-shaped morphology, in accordance with the normal morphological features of FLSs. Analysis of the expression of vimentin indicated that the cells derived from synovial tissues were FLSs.

3.2. BMP9 expression was significantly downregulated in RA FLSs

The expression levels of BMP9 in FLSs from the rats in the normal and AA groups were measured. Immunohistochemical and Western blotting analyses showed that the expression of BMP9 was downregulated observably in the RA synovial tissues, compared to that in the OA (control) tissues (Fig. 2A and B). Furthermore, immunohistochemistry was also used to analyze the expression of BMP9 in synovial tissues from normal rats and rats with AA, and the results showed that the expression of BMP9 was significantly decreased in the AA synovial tissues (Fig. 2C). Immunofluorescence staining showed that BMP9 protein expression was lower in the AA FLSs than in the normal FLSs (Fig. 2D). Likewise, Western blotting and q-PCR analyses demonstrated that the BMP9 protein and mRNA levels were clearly downregulated in FLSs isolated from AA rat synovial tissues (Fig. 2E and F). Thus, these results suggest that the expression of BMP9 was significantly reduced in AA FLSs.

3.3. BMP9-RNAi increases the proliferation and migration of FLSs

To explore additional evidence supporting the fact that BMP9 is involved in the proliferation and migration of RA FLSs, specific rat siRNA was used to knockdown the gene expression of BMP9 in AA FLSs. Normal and AA FLSs were transfected with control siRNA (NC-RNAi) or BMP9-RNAi (100 nM), and then cultured for 48 h following the transfection. The BMP9 protein and mRNA levels were reduced remarkably, compared to the cells transfected with NC-RNAi (Fig. 3A and B). As expected, the Western blot and q-PCR results showed that the protein and mRNA expression levels of c-Myc and Cyclin D1 were upregulated observably in normal and AA FLSs following transfection with BMP9 siRNA (Fig. 3A and B). Similarly, the cell cycle analysis also indicated that the treatment of AA FLSs with BMP9-RNAi resulted in an increase in the number of cells in the G2/M phase (Fig. 3C). In addition, the

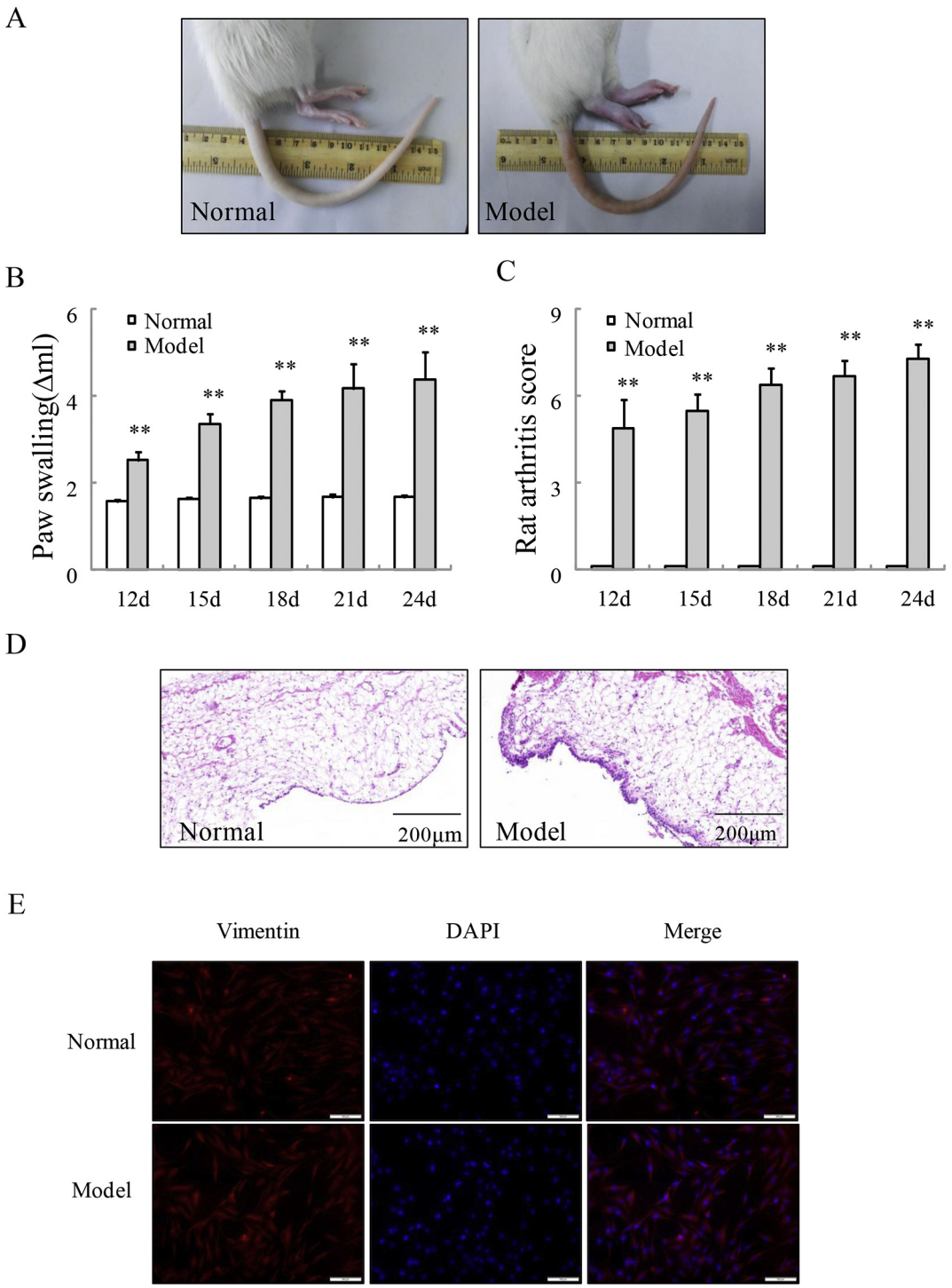

Fig. 1. The adjuvant-induced arthritis rat model was established.
(A) Images of representative paws of normal rats and rats with AA on day 24 after CFA induction. (B) The swelling of ankle joints was quantified with a plethysmometer. (C) Arthritis scores showed marked increases in rats from the model group. All values are expressed as the mean ± S.D. $^{**}P < 0.01$ vs normal group. (D) Representative H&E staining of AA and normal rat synovial tissues (original magnification, ×10). (E) Synovial cells of rats from the normal and model groups were identified by detecting vimentin using the immunofluorescence technique (original magnification, ×10).

protein and mRNA expression levels of MMP-2 and MMP-9 were upregulated remarkably following the transfection of the FLSs with BMP9 siRNA. Conversely, TIMP-1 was notably downregulated in normal and AA FLSs (Fig. 3D and E). The results of the wound-healing assay suggested that the migration ability of AA FLSs was notably promoted following their transfection with BMP9-RNAi (Fig. 3F). Thus, these results demonstrated that the inhibition of BMP9 expression could increase the proliferation and migration of FLSs from AA rats, and may participate in the progression of RA.

3.4. Transfection with the BMP9 overexpression vector inhibits the proliferation and migration of FLSs

In order to further determine the mechanism underlying the role of

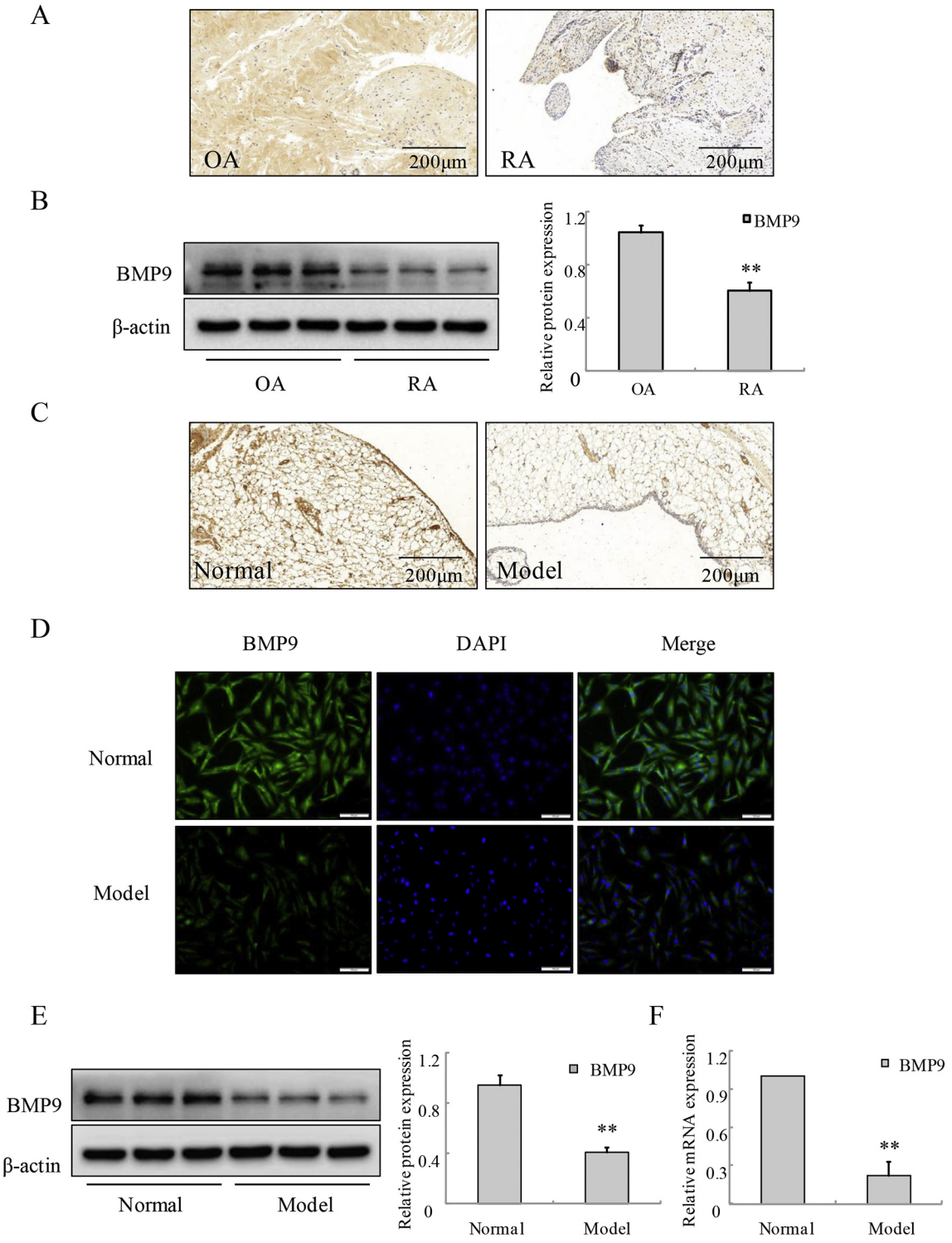

Fig. 2. The expression of BMP9 was downregulated in RA FLSs.
(A) The expression of BMP9 in human RA and OA synovial tissues was analyzed by IHC staining (original magnification, ×10). (B) The expression of BMP9 in normal and AA rat synovial tissues was analyzed by IHC staining (original magnification, ×10). (C) The protein levels of BMP9 in human RA and OA synovial tissues were analyzed by Western blotting. (D) The expression of BMP9 in FLSs from AA and normal rats was analyzed by immunofluorescence staining. (E) The protein levels of BMP9 in AA and normal FLSs were analyzed by Western blotting. (F) The mRNA levels of BMP9 in AA and normal FLSs were analyzed by Q-PCR. All values are expressed as the mean ± S.D. $^{**}P < 0.01$ vs normal group.

BMP9 in the proliferation and migration of FLSs, the overexpression vector PEX-3-BMP9 was used for overexpressing BMP9 in the FLSs of rats with AA. The Western blotting and Q-PCR (Fig. 4A and B) results suggested that the expression of BMP9 was upregulated remarkably following PEX-3-BMP9 transfection in normal and AA FLSs. Moreover, after transfection with PEX-3-BMP9, the protein and mRNA expression levels of c-Myc and Cyclin D1 were downregulated observably in normal and AA FLSs (Fig. 4A and B). As expected, FCM analysis suggested that BMP9 overexpression by transfection with PEX-3-BMP9 resulted in a significant decrease in the number of normal and AA FLSs

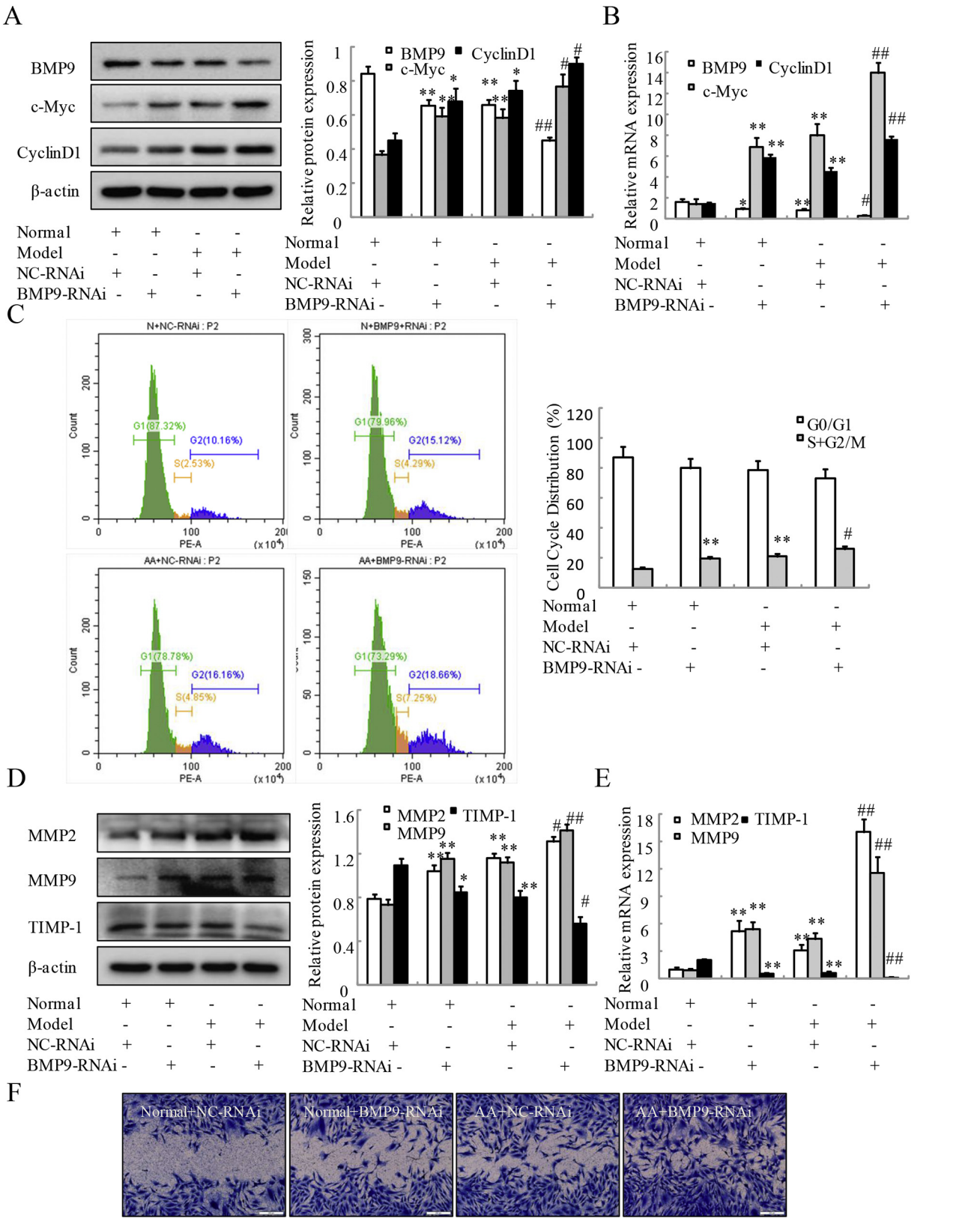

Fig. 3. BMP9 siRNA silencing increases the proliferation and migration of FLSs.
(A) The protein levels of BMP9, c-Myc, and Cyclin D1 in FLSs transfected with BMP9 siRNA were analyzed by Western blotting. (B) The mRNA levels of BMP9, c-Myc, and Cyclin D1 in FLSs transfected with BMP9 siRNA were analyzed by Q-PCR. (C) Cell cycle analysis of FLSs transfected with BMP9 siRNA for 48 h using FACS. (D) The protein levels of MMP-2, MMP-9, and TIMP-1 in FLSs transfected with BMP9 siRNA were analyzed by Western blotting. (E) The mRNA levels of MMP-2, MMP-9, and TIMP-1 in FLSs transfected with BMP9 siRNA were analyzed by Q-PCR. (F) FLSs were transfected with BMP9 siRNA, and their migration into the wound-healing site after 24 h was photographed (original magnification, ×10). All values are expressed as the mean ± S.D. $^{*}P < 0.05$, $^{**}P < 0.01$ vs normal group. $^{\#}P < 0.05$, $^{\#\#}P < 0.01$ vs model group.

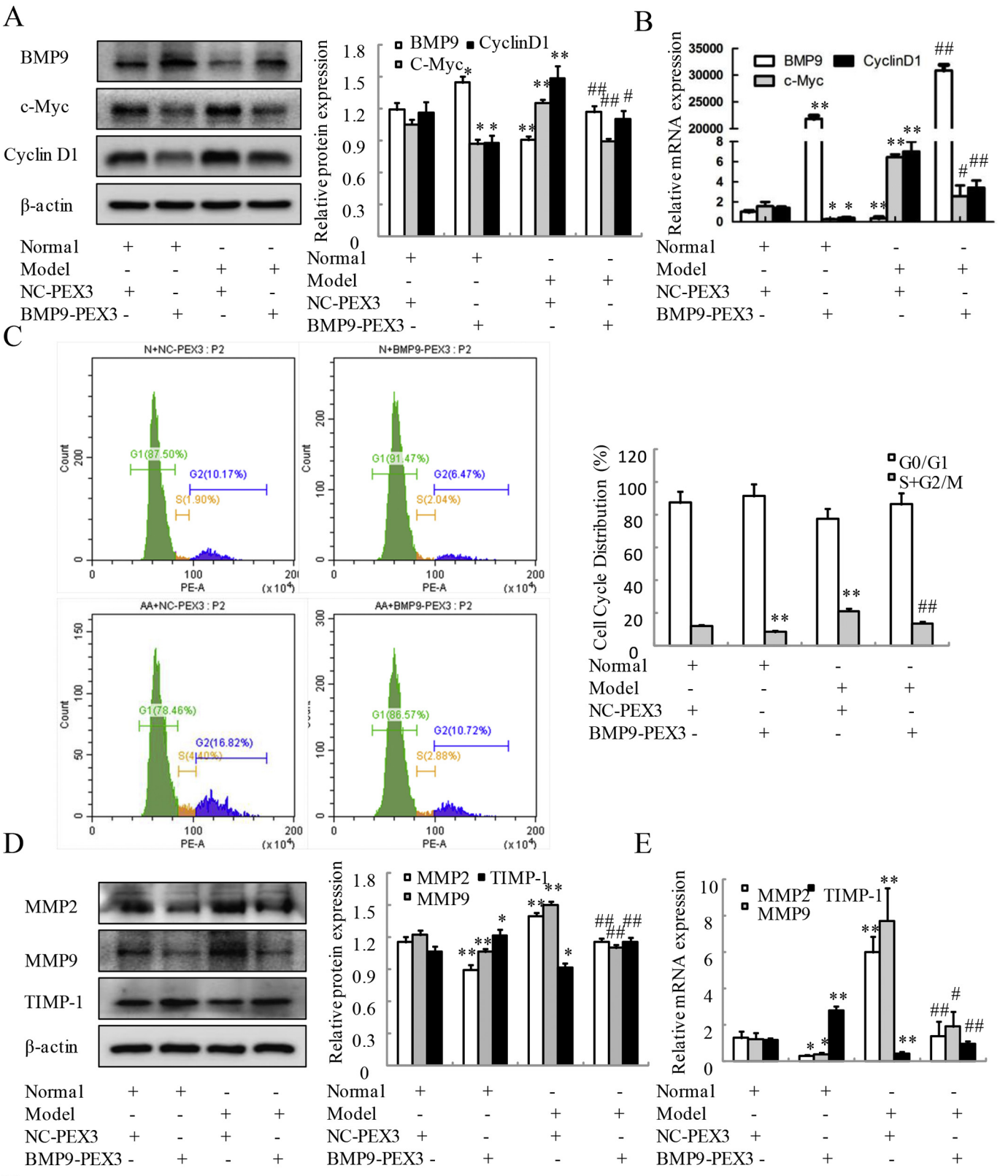

(caption on next page)

Fig. 4. BMP9 overexpression following transfection with the vector PEX-3-BMP9 inhibits the proliferation and migration of FLSs.
(A) The protein levels of BMP9, c-Myc, and Cyclin D1 in FLSs transfected with PEX-3-BMP9 were analyzed by Western blotting. (B) The mRNA levels of BMP9, c-Myc, and Cyclin D1 in FLSs transfected with PEX-3-BMP9 were analyzed by Q-PCR. (C) Cell cycle analysis of FLSs transfected with PEX-3-BMP9 for 48 h using FACS. (D) The protein levels of MMP-2, MMP-9, and TIMP-1 in FLSs transfected with PEX-3-BMP9 were analyzed by Western blotting. (E) The mRNA levels of MMP-2, MMP-9, and TIMP-1 in FLSs transfected with PEX-3-BMP9 were analyzed by Q-PCR. (F) FLSs were transfected with PEX-3-BMP9, and their migration into the wound-healing site after 24 h was photographed (original magnification, ×10). All values are expressed as the mean ± S.D. $^{*}P < 0.05$, $^{**}P < 0.01$ vs normal group. $^{\#}P < 0.05$, $^{\#\#}P < 0.01$ vs model group.

in the S phase and G2/M phase (Fig. 4C). Meanwhile, the protein and mRNA expression levels of MMP-2 and MMP-9 were also downregulated markedly following PEX-3-BMP9 transfection, whereas those of TIMP-1 were upregulated significantly (Fig. 4D and E). In addition, the wound-healing assay showed that the migration of normal and AA FLSs was markedly suppressed following BMP9 overexpression (Fig. 4F). These evidences indicated that the transfection of FLSs with PEX-3-BMP9 had an inhibitory effect on their proliferation and migration. Thus, BMP9 may play a vital role in the pathogenesis of RA.

3.5. BMP9 modulates the proliferation and migration of FLSs and may be associated with the AKT signaling pathway

BMP9 is known to be closely associated with the AKT signaling pathway in pathophysiological processes [24]. To investigate the effect of BMP9 on the AKT signaling pathway in FLSs, we measured the protein levels of phosphorylated (p)-AKT, a major component of the PI3K/AKT pathway, in FLSs transfected with PEX-3-BMP9 or BMP9-RNAi. Western blotting analysis indicated the clear upregulation of p-AKT in AA FLSs, compared to the FLSs from normal rats. In particular, the expression of p-AKT was significantly enhanced following BMP9 silencing, but reduced following BMP9 overexpression (Fig. 5A and B). These results indicated that BMP9 could modulate the proliferation and migration of FLSs, which may be closely associated with the AKT signaling pathway.

4. Discussion

The results of this study show that: 1) BMP9 expression was downregulated substantially in RA synovial tissues and AA FLSs; 2) BMP9-RNAi increased the proliferation and migration of AA FLSs; 3) the overexpression vector PEX-3-BMP9 suppressed the proliferation and migration of AA FLSs; and 4) BMP9 modulated the proliferation and migration of FLSs and may be closely associated with the AKT signaling pathway.

The AA rat is a well-established and widely used experimental model to study the pathophysiology of RA [25,26]; AA has characteristics similar to those of RA from the perspectives of histology and immunology, and is a useful test system for evaluating therapies for RA [27]. Hence, we chose AA to study the role of BMP9. RA is a chronic, systemic, autoimmune inflammatory disease that primarily attacks the synovial joints, leading to articular destruction and functional disability [7,28]. Excessive proliferation of FLSs is one of the critical features of RA, leading to cartilage and bone destruction [29]. Above all, the hyperplastic FLSs potentially promote lymphocyte and macrophage infiltration [30], recruitment, and retention via the production of chemokines [31], cytokines [32], cell adhesion molecules [33], and extracellular matrix proteins [30]. The migration of activated FLSs into the cartilage and bone is a critical event during invasive pannus formation in the RA synovium [34]. However, there are no approved drugs known for targeting FLSs in RA, and the mechanisms underlying the activation of FLSs remain unresolved. Thus, the inhibition of the proliferation and migration of FLSs may be an ideal target for the treatment of RA.

BMP9, a member of the BMP family, is involved in bone morphogenesis, functional differentiation, glucose homeostasis, and angiogenesis, and has been shown to be a pleiotropic cytokine [35]. Accumulated evidence has indicated that BMP9 plays an important role in regulating the proliferation, migration, differentiation, and apoptosis of various types of cells [14,36]. Herein, we explored whether BMP9 plays a role in regulating the proliferation and migration of AA FLSs. The Western blot and qRT-PCR analyses revealed that the expression of BMP9 was clearly reduced in AA FLSs, compared to normal FLSs. Moreover, immunohistochemical and immunofluorescence analysis also suggested that the expression of BMP9 in AA FLSs was lower than that in normal FLSs. Furthermore, the inhibition of BMP9 expression using BMP9 siRNA could activate the overexpression of the proto-oncogene c-Myc, Cyclin D1, and the MMPs MMP-2 and MMP-9, whereas TIMP-1 was downregulated. Furthermore, Cyclin D1 and c-Myc have been proven to be related to cell proliferation [37]. In addition, numerous experimental and clinical studies have indicated that the expression of MMP-2 and MMP-9, which comprise a family of zinc-dependent endopeptidases, provide suitable conditions for cell migration and invasion [38,39]. Conversely, the action of all MMPs is regulated by a group of endogenous TIMPs. More significantly, the results of the cell cycle analysis and wound-healing assay also suggested that the inhibition of BMP9 expression increased the proliferation and migration of FLSs from AA rats.

It is necessary to consider whether BMP9 overexpression could improve or regulate the proliferation and migration of FLSs. In our experiments, the transfection of FLSs from AA rats with the overexpression vector PEX-3-BMP9 had a profound inhibitory effect on their proliferation and migration. In this study, our results showed that BMP9 overexpression downregulated the expression of c-Myc, cyclin D1, MMP-2, and MMP-9, and upregulated the TIMP-1 expression. Thus, BMP9 overexpression significantly reduced the proliferation and migration of AA FLSs.

It is clear that BMP9 mediates cell activation by negatively regulating the PI3K/AKT signaling pathway [24,35]. The loss of BMP9 can result in the activation of p-AKT kinases, which play key roles in cell growth, proliferation, and invasion [24]. Our data also suggested that the inhibition of BMP9 by BMP9-RNAi significantly increased the p-AKT expression in AA FLSs. In particular, PEX-3-BMP9 suppressed AKT signaling, with a substantial decrease of p-AKT expression in AA FLSs. Collectively, these data indicated that BMP9 mediated the proliferation and migration of FLSs and might regulate the activation of the PI3K/AKT signaling pathway.

5. Conclusion

In this study, we found that BMP9 expression was significantly reduced in AA FLSs. BMP9 overexpression or silencing was associated with the proliferation and migration of FLSs. Additionally, the p-AKT expression was related to the BMP9 expression. The findings of the present study suggested that BMP9 may play a pivotal role in the proliferation and migration of FLSs through the activation of the AKT signaling pathway. Thus, we believe that BMP9 is a new target for the treatment of RA; these findings may potentially provide new ideas for studying RA.

Declaration of Competing Interest

The author has stated that there are no potential conflicts of interest in the research, authorship, and/or publication of this article.

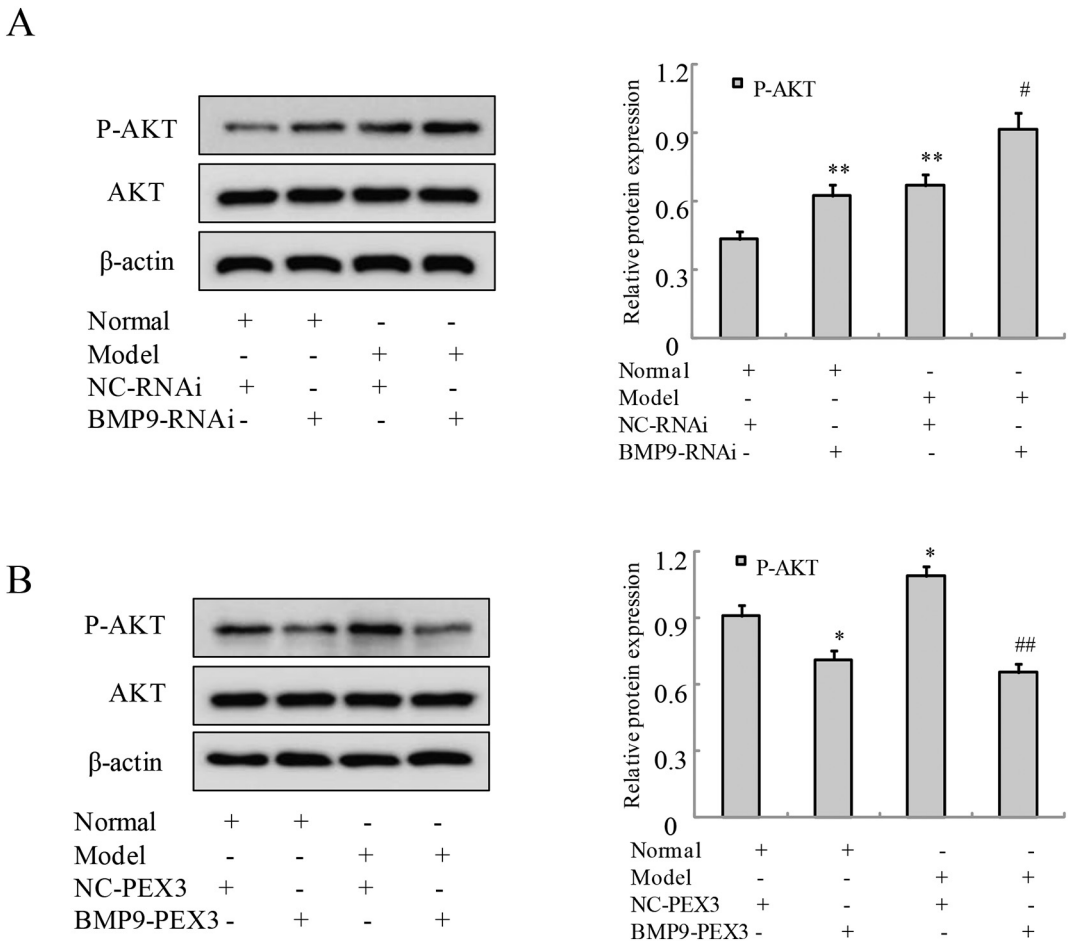

Fig. 5. BMP9 modulates the proliferation and migration of FLSs and may be closely associated with the AKT signaling pathway.
(A) The protein levels of p-AKT in FLSs transfected with BMP9 siRNA were analyzed by Western blotting. (B) The protein levels of p-AKT in FLSs transfected with PEX-3-BMP9 were analyzed by Western blotting. All values are expressed as the mean ± S.D. *P < 0.05, **P < 0.01 vs normal group. #P < 0.05, ##P < 0.01 vs model group.

Acknowledgements

This project was supported by the National Natural Science Foundation of China (No. 81770609).

References

[1] D.L. Scott, F. Wolfe, T.W. Huizinga, Rheumatoid arthritis, Lancet 376 (9746) (2010) 1094–1108.
[2] M. Kriegsmann, T.M. Randau, S. Gravius, K. Lisenko, C. Altmann, N. Arens, J. Kriegsmann, Expression of mi R-146a, mi R-155, and mi R-223 in formalin-fixed paraffin-embedded synovial tissues of patients with rheumatoid arthritis and osteoarthritis, Virchows Arch. 469 (1) (2016) 93–100.
[3] I.B. McInnes, G. Schett, The pathogenesis of rheumatoid arthritis, N. Engl. J. Med. 365 (23) (2011) 2205–2219.
[4] X. Jia, F. Wei, X. Sun, Y. Chang, S. Xu, X. Yang, C. Wang, W. Wei, CP-25 attenuates the inflammatory response of fibroblast-like synoviocytes co-cultured with BAFF-activated CD4(+) T cells, J. Ethnopharmacol. 189 (2016) 194–201.
[5] C.G. Miao, C. Huang, Y. Huang, Y.Y. Yang, X. He, L. Zhang, X.W. Lv, Y. Jin, J. Li, MeCP2 modulates the canonical Wnt pathway activation by targeting SFRP4 in rheumatoid arthritis fibroblast-like synoviocytes in rats, Cell. Signal. 25 (3) (2013) 598–608.
[6] N. Yeremenko, K. Zwerina, G. Rigter, D. Pots, J.E. Fonseca, J. Zwerina, G. Schett, D. Baeten, Tumor necrosis factor and interleukin-6 differentially regulate Dkk-1 in the inflamed arthritic joint, Arthritis Rheumatol 67 (8) (2015) 2071–2075.
[7] E.H. Noss, M.B. Brenner, The role and therapeutic implications of fibroblast-like synoviocytes in inflammation and cartilage erosion in rheumatoid arthritis, Immunol. Rev. 223 (2008) 252–270.
[8] B. Bartok, G.S. Firestein, Fibroblast-like synoviocytes: key effector cells in rheumatoid arthritis, Immunol. Rev. 233 (1) (2010) 233–255.
[9] M.R. Urist, Bone: formation by autoinduction. 1965, Clin. Orthop. Relat. Res. 395 (2002) 4–10.
[10] M.R. Urist, B.S. Strates, Bone morphogenetic protein, J. Dent. Res. 50 (6) (1971) 1392–1406.
[11] T. Katagiri, T. Watabe, Bone morphogenetic proteins, Cold Spring Harb. Perspect. Biol. 8 (6) (2016).
[12] F. Itoh, T. Watabe, K. Miyazono, Roles of TGF-beta family signals in the fate determination of pluripotent stem cells, Semin. Cell Dev. Biol. 32 (2014) 98–106.
[13] M. Kim, S. Choe, BMPs and their clinical potentials, BMB Rep. 44 (10) (2011) 619–634.
[14] D.O. Wagner, C. Sieber, R. Bhushan, J.H. Borgermann, D. Graf, P. Knaus, BMPs: from bone to body morphogenetic proteins, Sci. Signal. 3 (107) (2010) (mr 1).
[15] M. Daans, R.J. Lories, F.P. Luyten, Dynamic activation of bone morphogenetic protein signaling in collagen-induced arthritis supports their role in joint homeostasis and disease, Arthritis Res Ther 10 (5) (2008) R115.
[16] P.C. Verschueren, R.J. Lories, M. Daans, I. Theate, P. Durez, R. Westhovens, F.P. Luyten, Detection, identification and in vivo treatment responsiveness of bone morphogenetic protein (BMP)-activated cell populations in the synovium of patients with rheumatoid arthritis, Ann. Rheum. Dis. 68 (1) (2009) 117–123.
[17] M. Chemel, R. Brion, A.I. Segaliny, A. Lamora, C. Charrier, B. Brulin, Y. Maugars, B. Le Goff, D. Heymann, F. Verrecchia, Bone morphogenetic protein 2 and transforming growth factor beta 1 inhibit the expression of the proinflammatory cytokine IL-34 in rheumatoid arthritis synovial fibroblasts, Am. J. Pathol. 187 (1) (2017) 156–162.
[18] H.H. Luu, W.X. Song, X. Luo, D. Manning, J. Luo, Z.L. Deng, K.A. Sharff, A.G. Montag, R.C. Haydon, T.C. He, Distinct roles of bone morphogenetic proteins in osteogenic differentiation of mesenchymal stem cells, J. Orthop. Res. 25 (5) (2007) 665–677.
[19] Z. Lv, D. Yang, J. Li, M. Hu, M. Luo, X. Zhan, P. Song, C. Liu, H. Bai, B. Li, Y. Yang, Y. Chen, Q. Shi, Y. Weng, Bone morphogenetic protein 9 overexpression reduces osteosarcoma cell migration and invasion, Mol Cells 36 (2) (2013) 119–126.
[20] T. Wang, Z. Zhang, K. Wang, J. Wang, Y. Jiang, J. Xia, L. Gou, M. Liu, L. Zhou, T. He, Y. Zhang, Inhibitory effects of BMP9 on breast cancer cells by regulating their interaction with pre-adipocytes/adipocytes, Oncotarget 8 (22) (2017) 35890–35901.
[21] L. Gou, M. Liu, J. Xia, Q. Wan, Y. Jiang, S. Sun, M. Tang, L. Zhou, T. He, Y. Zhang, BMP9 promotes the proliferation and migration of bladder Cancer cells through up-

regulating lnc RNA UCA1, Int. J. Mol. Sci. 19 (4) (2018).
[22] M. Garcia-Alvaro, A. Addante, C. Roncero, M. Fernandez, I. Fabregat, A. Sanchez, B. Herrera, BMP9-induced survival effect in liver tumor cells requires p38MAPK activation, Int. J. Mol. Sci. 16 (9) (2015) 20431–20448.
[23] X. Chen, M. Orriols, F.J. Walther, E.H. Laghmani, A.M. Hoogeboom, A.C.B. Hogen-Esch, P.S. Hiemstra, G. Folkerts, M.T.H. Goumans, P. Ten Dijke, N.W. Morrell, G.T.M. Wagenaar, Bone morphogenetic protein 9 protects against neonatal hyperoxia-induced impairment of alveolarization and pulmonary inflammation, Front. Physiol. 8 (2017) 486.
[24] W. Ren, Y. Liu, S. Wan, C. Fei, W. Wang, Y. Chen, Z. Zhang, T. Wang, J. Wang, L. Zhou, Y. Weng, T. He, Y. Zhang, BMP9 inhibits proliferation and metastasis of HER2-positive SK-BR-3 breast cancer cells through ERK1/2 and PI3K/AKT pathways, PLoS One 9 (5) (2014) e96816.
[25] W.B. van den Berg, Lessons from animal models of arthritis over the past decade, Arthritis Res Ther 11 (5) (2009) 250.
[26] U. Snekhalatha, M. Anburajan, B. Venkatraman, M. Menaka, Evaluation of complete Freund's adjuvant-induced arthritis in a Wistar rat model. Comparison of thermography and histopathology, Z. Rheumatol. 72 (4) (2013) 375–382.
[27] X.F. Li, Y.Y. Sun, J. Bao, X. Chen, Y.H. Li, Y. Yang, L. Zhang, C. Huang, B.M. Wu, X.M. Meng, J. Li, Functional role of PPAR-gamma on the proliferation and migration of fibroblast-like synoviocytes in rheumatoid arthritis, Sci. Rep. 7 (1) (2017) 12671.
[28] G.S. Firestein, Evolving concepts of rheumatoid arthritis, Nature 423 (6937) (2003) 356–361.
[29] T. Pap, W.H. van der Laan, K.R. Aupperle, R.E. Gay, J.H. Verheijen, G.S. Firestein, S. Gay, M. Neidhart, Modulation of fibroblast-mediated cartilage degradation by articular chondrocytes in rheumatoid arthritis, Arthritis Rheum. 43 (11) (2000) 2531–2536.
[30] T.J. Smeets, E.C. Barg, M.C. Kraan, M.D. Smith, F.C. Breedveld, P.P. Tak, Analysis of the cell infiltrate and expression of proinflammatory cytokines and matrix metalloproteinases in arthroscopic synovial biopsies: comparison with synovial samples from patients with end stage, destructive rheumatoid arthritis, Ann. Rheum. Dis. 62 (7) (2003) 635–638.
[31] D.G. Lee, J.W. Woo, S.K. Kwok, M.L. Cho, S.H. Park, MRP8 promotes Th17 differentiation via upregulation of IL-6 production by fibroblast-like synoviocytes in rheumatoid arthritis, Exp. Mol. Med. 45 (2013) e20.
[32] H. Larsen, B. Muz, T.L. Khong, M. Feldmann, E.M. Paleolog, Differential effects of Th1 versus Th2 cytokines in combination with hypoxia on HIFs and angiogenesis in RA, Arthritis Res Ther 14 (4) (2012) R180.
[33] S.J. Park, K.J. Kim, W.U. Kim, C.S. Cho, Interaction of mesenchymal stem cells with fibroblast-like synoviocytes via cadherin-11 promotes angiogenesis by enhanced secretion of placental growth factor, J. Immunol. 192 (7) (2014) 3003–3010.
[34] Y.H. Huh, G. Lee, K.B. Lee, J.T. Koh, J.S. Chun, J.H. Ryu, HIF-2alpha-induced chemokines stimulate motility of fibroblast-like synoviocytes and chondrocytes into the cartilage-pannus interface in experimental rheumatoid arthritis mouse models, Arthritis Res Ther 17 (2015) 302.
[35] B. Li, Y. Yang, S. Jiang, B. Ni, K. Chen, L. Jiang, Adenovirus-mediated overexpression of BMP-9 inhibits human osteosarcoma cell growth and migration through downregulation of the PI3K/AKT pathway, Int. J. Oncol. 41 (5) (2012) 1809–1819.
[36] A.H. Reddi, A. Reddi, Bone morphogenetic proteins (BMPs): from morphogens to metabologens, Cytokine Growth Factor Rev. 20 (5–6) (2009) 341–342.
[37] H. Wu, J. Tao, X. Li, T. Zhang, L. Zhao, Y. Wang, L. Zhang, J. Xiong, Z. Zeng, N. Zhan, C.J. Steer, L. Che, M. Dong, X. Wang, J. Niu, Z. Li, G. Yan, X. Chen, G. Song, Micro RNA-206 prevents the pathogenesis of hepatocellular carcinoma by modulating expression of met proto-oncogene and cyclin-dependent kinase 6 in mice, Hepatology 66 (6) (2017) 1952–1967.
[38] S.Y. Bae, H.J. Kim, K.J. Lee, K. Lee, Translationally controlled tumor protein induces epithelial to mesenchymal transition and promotes cell migration, invasion and metastasis, Sci. Rep. 5 (2015) 8061.
[39] S. Zou, J. Yang, J. Guo, Y. Su, C. He, J. Wu, L. Yu, W.Q. Ding, J. Zhou, RAD18 promotes the migration and invasion of esophageal squamous cell cancer via the JNK-MMPs pathway, Cancer Lett. 417 (2018) 65–74.